2 Blood–Brain Barrier and Blood–CSF Barrier Function

H. Reiber

The restriction of free exchange of molecules and cells between the blood and the perivascular extracellular spaces is referred to as a "barrier." Passage rates may vary greatly because of the different morphological structures, but all molecules, including the largest proteins, and entire cells can pass these structures, even the blood–brain barrier with its particularly tight intercellular junctions.

Blood–Brain Barrier

Structure. The blood–brain barrier is a morphologically defined structure. Its special components include capillaries, the basal membrane, and a perivascular layer of astroglial cells. Unlike other capillaries, some brain capillaries have an endothelium with cells connected by tight junctions. The tight junctions around brain capillary cells form a three-dimensional maze, which is not as impenetrable as their morphology in two-dimensional tissue sections suggests. In addition, the capillary structures in brain are not uniform but also contain fenestrated capillaries. All these morphological features are sufficient to explain the passage of large particles by passive diffusion from blood to brain and CSF. However, it is neither morphologically nor functionally justified to refer to any of these passageways as "pores."

Permeability. The permeability and selectivity of the blood–brain barrier for proteins is determined by the diffusion of the macromolecules, which is dependent on molecular size. Properly speaking, what we are speaking of is a particular barrier function *for proteins*, as distinct from other facilitated or active transfer processes for other molecules—for in fact a variety of different barrier functions exist based on the different conditions of passage for different classes of substances, e.g., amino acids (Kruse et al., 1985), sugars, and vitamins (Reiber et al., 1993).

The Blood–CSF Barrier Function

Definition

It is the blood–*CSF* barrier function which is the really important function in CSF analysis. Empirically, it is described by the ratio of protein concentrations in venous blood and (lumbar) CSF. Unlike the blood–brain barrier, it includes dynamic aspects (e.g., CSF flow) that cannot be described in morphological terms (Reiber, 1994 a).

A blood-derived protein, such as albumin, reaches the CSF via diffusion from local blood vessels directly into the ventricles, the cisterns, and the cerebral and spinal subarachnoid spaces. Thus, its concentration increases steadily along the pathway of CSF flow, and hence also (secondarily—Reiber, 2003) depends on the flow rate (**Fig. 2.1**).

The multiplicity of morphological structures restricting the diffusion of molecules between blood and CSF, and the additional functional effects of CSF flow rate on CSF protein concentrations, have given rise to the term blood–CSF barrier *function*.

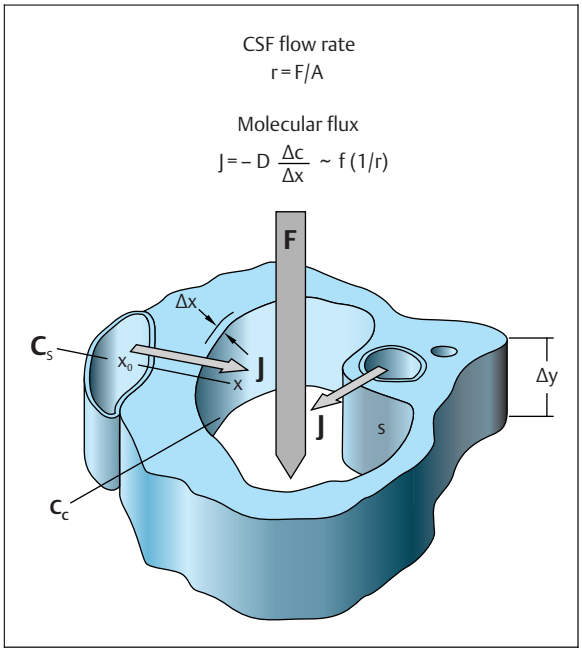

Fig. 2.1 Contributions of diffusion and CSF flow to blood–CSF barrier function. Molecules in serum at a concentration C_S diffuse through the tissue along the diffusion pathway (x) into the CSF of the subarachnoid space (concentration in CSF: C_L). The molecular flux J depends on the local concentration gradient $\Delta c/\Delta x$ or dc/dx and the diffusion coefficient D (Fick's First Law). When the CSF flow rate decreases (and thus also the volume turnover), the molecular flux, which remains steady, enters a smaller volume, and thus the concentration of proteins in the CSF rises. As the concentrations (C_L) change, the local gradient (dc/dx) changes as well (Fick's Second Law). This is why the bulk CSF flow rate (F) has a nonlinear influence on blood-derived proteins in CSF—that is, on the blood–CSF barrier function. The flow rate of a molecule in the CSF is $r = F/A$, with A being the variable cross-section of the subarachnoid space volume fraction, $\Delta s, = A \cdot \Delta y$. J has a reciprocal relation to the flow rate of a molecule in CSF, r.

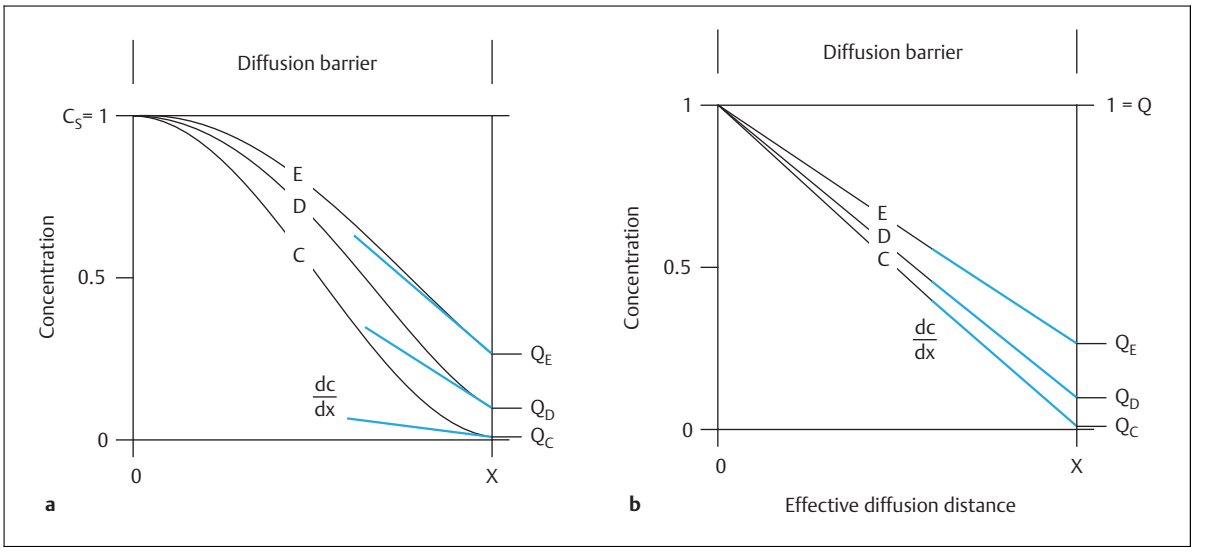

Fig. 2.2 a, b Dynamics of blood-derived proteins between blood and CSF before (curve *C*) and after (curves *D* and *E*) pathological reduction of the CSF flow rate. Comparison of the nonlinear model (**a**) with the linear model (**b**) of the blood/CSF protein concentration gradient. The serum concentration (C_S) of an individual protein has been normalized, its maximum value being $C_S = 1$. Corresponding CSF concentrations are presented as dimension-free CSF/serum quotients (Q_C, Q_D, Q_E) with values ranging between 0 and 1. The idealized diffusion barrier is illustrated as the effective diffusion distance (*x*) (Reiber, 1994 a). As the CSF flow rate drops (from *C* to *E*), the protein concentration rises (e. g., IgM). The calculated overall ratio between blood and CSF concentrations is the same in **a** and **b**, but in **a** the local concentration gradient (dc/dx) at the border with the subarachnoid space (at *x*) increases in curves *C* to *E*, due to the increasing mean penetration depth (Reiber, 1994 a), whereas in the linear model (**b**) it decreases. The molecular flux *J* (**Fig. 2.1**) increases nonlinearly from *C* to *E* (**a**), whereas it would decrease linearly from *C* to *E* in model **b**. Only the nonlinear model can give a quantitative explanation of the empirically observed nonlinear increase in CSF protein concentration as CSF flow rate drops and Q_{Alb} increases (**Figs. 2.4** and **2.5**).

The blood–brain barrier is defined in morphological terms, whereas the blood–CSF barrier is defined in terms of function: after all, CSF protein concentrations are measured a long way away from the actual "barrier"—after a long CSF pathway with constant opportunities for exchange—and then related to the serum concentration in venous blood.

Biophysical Model of Blood–CSF Barrier Function

Comparison with earlier models. The new paradigm of blood–CSF barrier function and dysfunction was derived from the laws of diffusion (Reiber, 1994 a, 1994 b). It replaces many linear and nonlinear empirical data fits that were not supported by any physiological or biophysical theory (for references see Reiber, 1994 a). The essential difference of the new paradigm from earlier models, which assumed that the overall concentration gradient between blood and CSF was linear (**Fig. 2.2 b**), is that it assumes a nonlinear concentration gradient between blood and CSF, with a steady state between molecular diffusion and CSF flow rate (**Figs. 2.1, 2.2 a**). In this molecular flux/CSF flow model, proteins diffusing from the blood through the tissue into the CSF are eliminated by bulk flow with the passing CSF, and these two processes create a dynamic equilibrium—a steady state. Without CSF flow, the protein concentration in CSF would gradually approach the serum concentration (as it does in a corpse shortly after death, when CSF flow ceases).

Protein concentrations in CSF. The sigmoid change in tissue concentration along the diffusion barrier from the blood into the CSF (**Fig. 2.2 a**) is determined by:

- Diffusion.
- CSF flow rate.

The rate of protein diffusion into the CSF space—the molecular flux (*J* in **Fig. 2.1**)—depends on:

- The size of the protein molecules (**Table 3.1**).
- The local concentration gradient at the border between endothelium and subarachnoid space.

It is important for the mathematical treatment that the local concentration gradient (dc/dx) (**Fig. 2.2 a**) at the endothelial surface(s) facing the subarachnoid space is used (Reiber, 1994 a), rather than the (linear) overall concentration gradient between blood and CSF (**Fig. 2.2 b**).

The crucial point of the theory—particularly for the evaluation of pathological processes—is that the slope of the local concentration gradient is affected by the CSF flow rate, and in a nonlinear way.

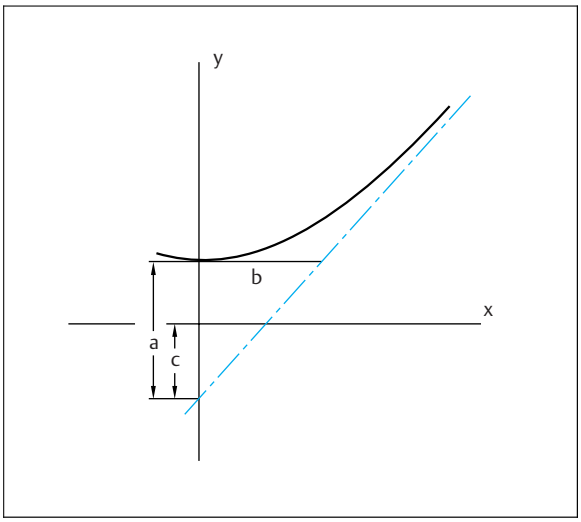

Fig. 2.3 Hyperbolic function. The figure shows one of four branches of a complete hyperbolic function: $y = a/b(x^2-y^2)^{0.5} - c$, where a/b is the slope of the asymptote and c the coordinate transformation of the y-axis (the intersection of the asymptotes is not identical with the origin of the diagram).

With this discovery it became possible to derive a hyperbolic function (**Fig. 2.3**) for the description of the relationship between CSF concentrations of molecules of different sizes—for example, between Q_{IgG} and Q_{Alb} (**Figs. 2.4, 2.5**). **Figure 2.4** shows an example of hyperbolic functions for a fraction of the empirical data collected from 4300 patients (Reiber, 1994 a) as a basis for the establishing of the reference values in the CSF/serum quotient diagrams (Reiber and Peter, 2001). This *diffusion/CSF flow theory* requires no assumptions to be made about the morphology of the structures participating in the blood–CSF barrier function, since the same diffusion conditions apply for all molecules whose ratio during passage is being considered. The molecular-size-dependent "selectivity" for the passage of blood proteins into the CSF space (**Table 3.1**) is fully explained by the molecular-size-dependent diffusion coefficient.

Impact of the CSF Flow Rate

Decreasing CSF flow rate. A pathologically reduced CSF flow rate has the following consequences (Reiber, 1994 a):

- The protein concentration in the CSF increases as a primary consequence, because the volume turnover is reduced but the molecular flux J remains constant (**Figs. 2.1, 2.2 a**). Q_C thus becomes Q_D (**Fig. 2.2 a**).
- As the result of the higher concentration in the CSF, the mean concentration in the tissue also rises (curve C becomes curve D, **Fig. 2.2 a**).
- This in turn alters the local concentration gradient (dc/dx) in a nonlinear fashion, thus increasing the molecular flux J in a nonlinear fashion (Fick's Second Law).
- This facilitates the entrance of molecules into the subarachnoid space (for $Q_{Alb} < 0.5$) and causes a further (secondary) increase in protein concentration in the CSF until a new steady state is reached (curve E, **Fig. 2.2 a**).

Thus, this process contains a positive feedback mechanism—like autocatalysis—which enhances the effect of a process once begun. This nonlinearity is what distinguishes this model from earlier, linear models.

Hyperbolic function. If we now relate the concentration of two molecules of different sizes in CSF (e. g., Q_{IgG}/Q_{Alb}), their ratio to one another changes as CSF flow diminishes (and the protein concentration in the CSF increases) in accordance with the following function (Reiber, 1994 a):

$$Q_{IgG} = \frac{erfc\ (z\ \sqrt{D_{IgG}/D_{Alb}})}{erfc\ z} \cdot Q_{Alb}$$

This function has been recognized as a hyperbolic function (Reiber, 1994 a) in which the ratio of Q_{IgG}/Q_{Alb} depends entirely on the ratio of the diffusion coefficients (D_{IgG}/D_{Alb}). This equation, which uses complicated trigonometric series (error function complement, *erfc*) for the diffusion pathway (z), can now also be described by a common hyperbolic function (**Fig. 2.4**):

$$Q_{IgG} = a/b\ \sqrt{(Q_{Alb})^2 + b^2} - c$$

This is the function introduced earlier on a purely empirical basis (Reiber and Felgenhauer, 1987). Parameters a/b, b, and c (see **Table 5.3**) have now been improved by empirical fit of the data measured for IgG, IgA, and IgM in the CSF, using a larger study group (Reiber, 1994 a). This concept is valid for all blood-derived proteins in CSF (**Fig. 2.5**).

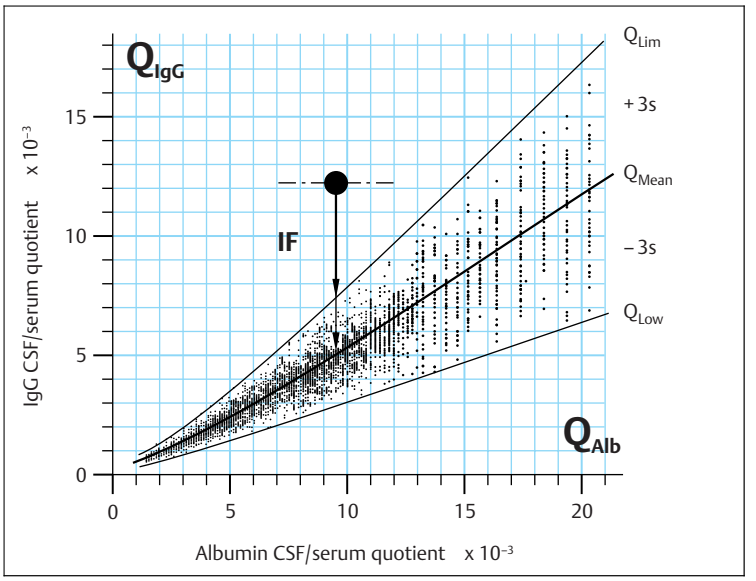

Fig. 2.4 CSF/serum quotients for IgG (Q_{IgG}) as a function of the albumin CSF/serum quotient (Q_{Alb}). The reference ranges of proteins in CSF that derive exclusively from blood have been determined from patients (n = 4154) without a humoral immune reaction (normal controls and patients with various neurological diseases). The range of reference values is characterized by the hyperbolic functions for Q_{Lim}, Q_{Mean}, and Q_{Low} shown in this figure, which represents a small fraction of the whole range with albumin quotients up to $Q_{Alb} = 150 \times 10^{-3}$. The corresponding parameters of the hyperbolic functions are reported in **Table 5.3**, for IgA and IgM as well as for IgG. In the diagnostic routine for detection of intrathecal IgG synthesis we discriminate between CNS-derived and blood-derived fractions in the CSF by reference to Q_{Lim}. In the figure, the intrathecal fraction (IF, upper arrow) is shown for the example of a patient with intrathecal IgG synthesis (large dot, with $Q_{Alb} = 10 \times 10^{-3}$ and $Q_{IgG} = 12.2 \times 10^{-3}$). When comparing groups of patients (disease group vs. control group) for statistical evaluation, it is more relevant to refer to Q_{Mean} as the mean of the control group (Reiber and Albaum, 2008). The quotient diagram, in particular the discrimination line Q_{Lim}, is valid for ventricular, cisternal, and lumbar CSF. Detection of a barrier dysfunction only requires the use of different age-related reference values for the albumin quotient (Chap. 21, "Proteins").

Rostrocaudal Concentration Gradient

The continuous diffusion of serum molecules into the CSF from the blood vessels along the CSF flow paths, e. g., along the spine, creates a rostrocaudal concentration gradient in the lumbar subarachnoid space. This gradient explains the observation that the diffusion of molecules from the blood into lumbar CSF is faster than their diffusion into ventricular CSF. The gradient is again nonlinear (Reiber, 2003). The increasing CSF concentration down the spine also induces an increasing concentration in the tissue (Reiber, 1994 a) and consequently an increase in the local concentration gradient going down the lumbar CSF space, to be understood as locally different steady states—as in a standing wave in acoustics, with locally different amplitudes.

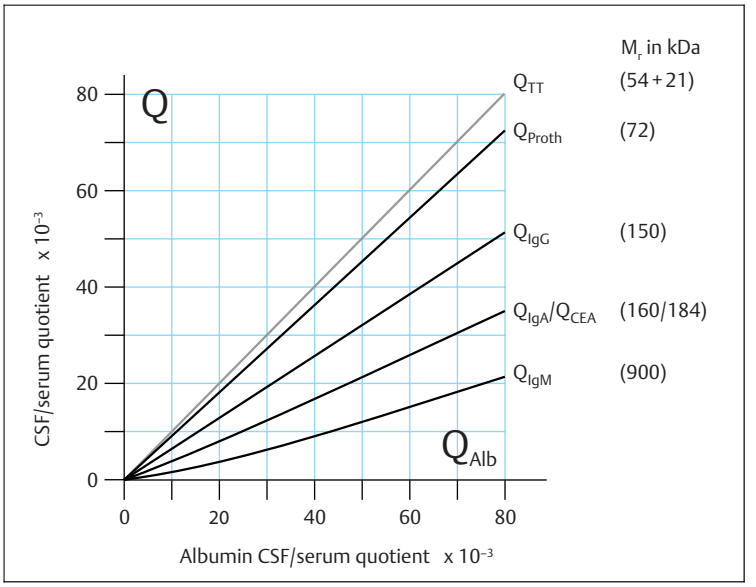

Fig. 2.5 Molecular-size-dependent changes in the mean CSF/serum quotients (Q) of serum proteins in CSF with diminishing CSF flow rate. The description of protein quotients as a function of the albumin quotient by means of a hyperbolic function is valid for IgG, IgA, and IgM, as well as for all other serum proteins in the CSF studied so far. Proteins with molecular sizes larger than that of albumin lie below the 45 ° line, and the larger the molecule, the less steep the slope of the line (see also **Table 3.1**). Transthyretin (TT, 54 kDa), which is associated with retinol-binding protein (RBP, 21 kDa), passes the barrier at nearly the same molecular size as albumin (67 kDa). Consequently, their quotient ratio follows a 45 ° line.

References

Kruse T, Reiber H, Neuhoff V. Amino acid transport across the human blood–CSF barrier. An evaluation graph for amino acid concentrations in cerebrospinal fluid. J Neurol Sci 1985;70:129–138

Reiber H. Flow rate of cerebrospinal fluid (CSF)—a concept common to normal blood–CSF barrier function and to dysfunction in neurological diseases. J Neurol Sci 1994 a;122:189–203.

Reiber H. The hyperbolic function: a mathematical solution of the protein flux/CSF flow model for blood–CSF barrier function J Neurol Sci 1994 b;126:240–242.

Reiber H. Proteins in cerebrospinal fluid and blood. Barriers, CSF flow rate and source-related dynamics. Restor Neurol Neurosci 2003;21:79–96.

Reiber H, Albaum W. Statistical evaluation of intrathecal protein synthesis in CSF/serum quotient diagrams. Acta Neuropsychiatr 2008; 20 (S 1):48–49 (www.comed-com.de)

Reiber H, Peter JB. Cerebrospinal fluid analysis—disease-related data patterns and evaluation programs. J Neurol Sci 2001;184:101–122.

Reiber H, Felgenhauer K. Protein transfer at the blood–CSF barrier and the quantitation of the humoral immune response within the central nervous system. Clin Chim Acta 1987;163:319–328

Reiber H, Ruff M, Uhr M. Ascorbate concentration in human cerebrospinal fluid (CSF) and serum. Intrathecal accumulation and CSF flow rate. Clin Chim Acta 1993;217:163–173